Voltage control of DC islanded microgrids

A decentralized scalable approach

Tucci, Michele; Riverso, Stefano; Quintero, Juan Carlos Vasquez; Guerrero, Josep M.; Ferrari-Trecate, Giancarlo

Published in:
54th IEEE Conference on Decision and Control

DOI (link to publication from Publisher):
10.1109/CDC.2015.7402691

Publication date:
2015

Document Version
Accepted author manuscript, peer reviewed version

Voltage control of DC islanded microgrids: a decentralized scalable approach

Michele Tucci, Stefano Riverso, *Member, IEEE*, Juan C. Vasquez, *Member, IEEE*,
Josep M. Guerrero, *Fellow, IEEE*, and Giancarlo Ferrari-Trecate, *Senior Member, IEEE*

***Abstract*— We propose a new decentralized control scheme for DC Islanded microGrids (ImGs) composed by several Distributed Generation Units (DGUs) with a general interconnection topology. Each local controller regulates to a reference value the voltage of the Point of Common Coupling (PCC) of the corresponding DGU. Notably, off-line control design is conducted in a Plug-and-Play (PnP) fashion meaning that (i) the possibility of adding/removing a DGU without spoiling stability of the overall ImG is checked through an optimization problem; (ii) when a DGU is plugged in or out at most neighbouring DGUs have to update their controllers and (iii) the synthesis of a local controller uses only information on the corresponding DGU and lines connected to it. This guarantee total scalability of control synthesis as the ImG size grows or DGUs gets replaced. Yet, under mild approximations of line dynamics, we formally guarantee stability of the overall closed-loop ImG. The performance of the proposed controllers is analyzed simulating different scenarios in PSCAD.**

I. Introduction

In the recent years, the increasing penetration of renewable energy sources has motivated a growing interest for microgrids, energy networks composed by the interconnection of DGUs and loads [1]. Microgrids are self-sustained electric systems that can supply local loads even in islanded mode, i.e. disconnected from the main grid [2]. So far, research mainly focused on AC microgrids [1], [2], [3], [4]. However, technological advances in power electronics converters have considerably facilitated the operation of DC power systems. This, together with the increasing use of DC renewables (e.g. PV panels), batteries and loads (e.g. electronic appliances, LEDs and electric vehicles), has triggered a major interest in DC microgrids [5], [6].

For AC ImGs a key issue is to guarantee voltage and frequency stability by controlling inverters interfacing energy sources with lines and loads. This problem has received great attention and several decentralized control schemes have been proposed [2], [7], [8], [3], [4]. Some control design approaches are scalable, meaning that the design of a local controller for a DGU is not based on the knowledge of the whole ImG and the complexity of local control design is independent of the ImG size. In particular, the method proposed in [3], [4] allows for the seamless plugging-in, unplugging and replacement of DGUs without spoiling ImG stability. Control design procedure with these features have been termed PnP [9], [10], [11], [12].

Voltage stability is critical also in DC microgrids as they cannot be directly coupled to an "infinite-power" source, such as the AC main grid, and therefore they always operate in islanded mode. Existing controllers for the stabilization of DC ImGs are mainly based on droop control [5], [13], [14] and stability analysis has been performed only for specific ImGs [5], [13], [14]. Similar approaches to voltage stabilization have been also used for multi-terminal high voltage DC systems [15].

In this paper we develop a totally scalable method for the synthesis of decentralized controllers for DC ImGs. In Section III, we propose a PnP design procedure where the synthesis of a local controller requires only the model of the corresponding DGU and the parameters of transmission lines connected to it. Importantly, no specific information about any other DGU is needed. Moreover, when a DGU is plugged in or out, only DGUs physically connected to it have to retune their local controllers. As in [3], we exploit Quasi-Stationary Line (QSL) approximations of line dynamics [16] and use structured Lyapunov functions for mapping control design into a Linear Matrix Inequality (LMI) problem. This also allows to automatically deny plugging in/out requests if these operations spoil the stability of the ImG.

In order to validate our results, we run several simulations in PSCAD using realistic models of Buck converters and associated filters.

II. Model of a DC Microgrid

This section discusses dynamic models of ImGs. For clarity, we start by introducing an ImG consisting of two parallel DGUs and then generalize it to N DGUs. Consider the scheme depicted in Figure 1 comprising two DGUs denoted with i and j and connected through a DC line with an impedance specified by parameters $R_{ij} > 0$ and $L_{ij} > 0$. At each DGU level, we represent a generic renewable resource through a DC voltage source. Moreover, a Buck converter is present in order to supply a local DC load connected to the PCC through a series LC filter. For instance, the DC load can be a combination of resistive electronic loads and negative resistance of constant power loads. We assume that loads are unknown and we treat them as current disturbances (I_L) [3], [17].

For $* \in \{i, j\}$, the model of DGU $*$ can be described as

M. Tucci and G. Ferrari-Trecate are with Dipartimento di Ingegneria Industriale e dell'Informazione, Università degli Studi di Pavia.

S. Riverso is with United Technologies Research Center Ireland, 4th Floor, Penrose Business Center, Penrose Wharf, Cork, Ireland.

J. C. Vasquez and J. M. Guerrero are with the Institute of Energy Technology, Aalborg University, Aalborg East DK-9220, Denmark.

michele.tucci02@universitadipavia.it, Corresponding author.

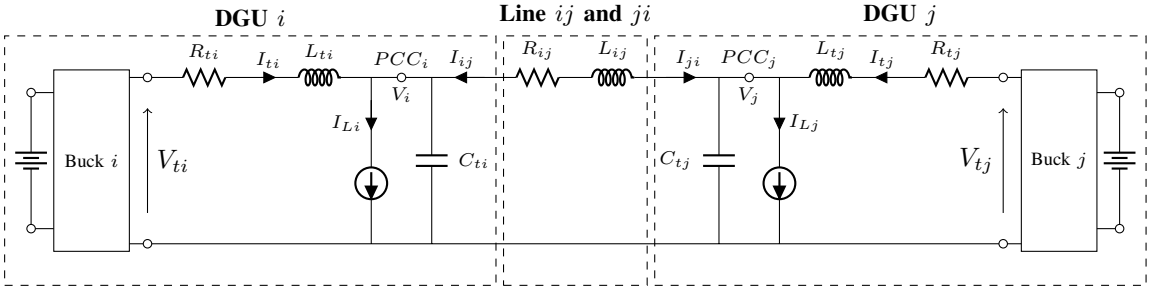

Fig. 1: Electrical scheme of an ImG composed of two parallel DGUs with unmodeled loads.

follows

$$\frac{dV_*}{dt} = \frac{1}{C_{t*}} I_{t*} + \frac{1}{C_{t*}} I_{*\circ} - \frac{1}{C_{t*}} I_{L*} \tag{1a}$$

$$\frac{dI_{t*}}{dt} = -\frac{R_{t*}}{L_{t*}} I_{t*} - \frac{1}{L_{t*}} V_* + \frac{1}{L_{t*}} V_{t*} \tag{1b}$$

where $\circ \in \{i, j\}$ and $\circ \neq *$. For the line $*\circ$, we obtain

$$\frac{dI_{*\circ}}{dt} = -\frac{R_{*\circ}}{L_{*\circ}} I_{*\circ} - \frac{1}{L_{*\circ}} V_* + \frac{1}{L_{*\circ}} V_\circ \tag{2}$$

As in [3], we notice that setting $* = i$ or $* = j$ in (2) translates into obtain two opposite line currents I_{ij} and I_{ji}. This is equivalent to have a reference current entering in each DGU. We exploit the following assumption to ensure that $I_{ij}(t) = -I_{ji}(t)$, $\forall t \geq 0$.

Assumption 1: Initial states for the line currents fulfill $I_{*\circ}(0) = -I_{\circ *}(0)$. Furthermore, we set $L_{*\circ} = L_{\circ *}$ and $R_{*\circ} = R_{\circ *}$.

In the following section, we show how to describe each DGU as a dynamical system affected directly by state of the other DGU connected to it.

A. QSL model

As in [16], we set $\frac{dI_{ij}}{dt} = 0$ and $\frac{dI_{ji}}{dt} = 0$. Consequently, from (2), one gets the QSL model

$$\bar{I}_{*\circ} = \frac{V_\circ}{R_{*\circ}} - \frac{V_*}{R_{*\circ}} \tag{3}$$

By replacing variable $I_{*\circ}$ in (1a) with the right-hand side of (3), we obtain the following model of DGU $*$ and we call it $\Sigma^{DGU}_{[*]}$

$$\begin{aligned} \dot{x}_{[*]}(t) &= A_{**} x_{[*]}(t) + B_* u_{[*]}(t) + M_* d_{[*]}(t) + \xi_{[*]}(t) \\ y_{[*]}(t) &= C_* x_{[*]}(t) \\ z_{[*]}(t) &= H_* y_{[*]}(t) \end{aligned} \tag{4}$$

where $x_{[*]} = [V_*, I_{t*}]^T$ is the state, $u_{[*]} = V_{t*}$ the control input, $d_{[*]} = I_{L*}$ the exogenous input and $z_{[*]} = V_*$ the controlled variable of the system. Moreover, $y_{[*]}(t)$ is the measurable output and we assume $y_{[*]} = x_{[*]}$, while $\xi_{[*]}(t) = A_{*\circ} x_{[\circ]}$ represents the coupling with DGU $\circ$. All the matrices of $\Sigma^{DGU}_{[*]}$ (obtained from (1) and (3)) are provided in Appendix A.2 of [18]. At this point, we notice that the model of DGU $*$ does not depend on the dynamics of the line which, however, are asymptotically stable by virtue of the positivity of the line parameters. Consequently, we can conclude that stability of the ImG depends on the stability of $\Sigma^{DGU}_{[i]}$ and $\Sigma^{DGU}_{[j]}$ interconnected through the QSL model (3). The resulting system is called QSL-ImG model.

B. QSL model of a microgrid composed of N DGUs

In this section, a generalization of model (4) to ImGs composed of N DGUs is presented. Let $\mathcal{D} = \{1, \ldots, N\}$. First, we call two DGUs neighbours if there is a transmission line connecting them. Then, we denote with $\mathcal{N}_i \subset \mathcal{D}$ the subset of neighbours of DGU i. We highlight that the neighbouring relation is symmetric, consequently $j \in \mathcal{N}_i$ implies $i \in \mathcal{N}_j$. In order to describe the dynamics of DGU i, we use model (4), with $\xi_{[i]} = \sum_{j \in \mathcal{N}_i} A_{ij} x_{[j]}(t)$. The new matrices of $\Sigma^{DGU}_{[i]}$ are collected in Appendix A.3 of [18], while the overall QSL-ImG model can be written as follows

$$\dot{\mathbf{x}}(t) = \mathbf{A}\mathbf{x}(t) + \mathbf{B}\mathbf{u}(t) + \mathbf{M}\mathbf{d}(t) \tag{5a}$$

$$\mathbf{y}(t) = \mathbf{C}\mathbf{x}(t) \tag{5b}$$

$$\mathbf{z}(t) = \mathbf{H}\mathbf{y}(t) \tag{5c}$$

where $\mathbf{x} = (x_{[1]}, \ldots, x_{[N]}) \in \mathbb{R}^{2N}$, $\mathbf{u} = (u_{[1]}, \ldots, u_{[N]}) \in \mathbb{R}^N$, $\mathbf{d} = (d_{[1]}, \ldots, d_{[N]}) \in \mathbb{R}^N$, $\mathbf{y} = (y_{[1]}, \ldots, y_{[N]}) \in \mathbb{R}^{2N}$, $\mathbf{z} = (z_{[1]}, \ldots, z_{[N]}) \in \mathbb{R}^N$. For the details of matrices $\mathbf{A}$, $\mathbf{B}$, $\mathbf{M}$, $\mathbf{C}$ and $\mathbf{H}$ we defer the reader to Appendix A.3 of [18].

III. Plug-and-Play decentralized voltage control

A. Decentralized control scheme with integrators

Let $\mathbf{z_{ref}}(t)$ denote the constant desired reference trajectory for the output $\mathbf{z}(t)$. In order to track asymptotically $\mathbf{z_{ref}}(t)$ when $\mathbf{d}(t)$ is constant, we consider the augmented ImG model with integrators. A necessary condition for having that the steady-state error $\mathbf{e}(t) = \mathbf{z_{ref}}(t) - \mathbf{z}(t)$ tends to zero as $t \to \infty$, is that for arbitrary constant signals $\mathbf{d}(t) = \bar{\mathbf{d}}$ and $\mathbf{z_{ref}}(t) = \bar{\mathbf{z}}_{\mathbf{ref}}$, there are equilibrium states and inputs $\bar{\mathbf{x}}$ and $\bar{\mathbf{u}}$ verifying

$$\begin{aligned} \mathbf{0} &= \mathbf{A}\bar{\mathbf{x}} + \mathbf{B}\bar{\mathbf{u}} + \mathbf{M}\bar{\mathbf{d}} \\ \bar{\mathbf{z}}_{\mathbf{ref}} &= \mathbf{H}\mathbf{C}\bar{\mathbf{x}} \end{aligned} \tag{6}$$

$$\Gamma \begin{bmatrix} \bar{\mathbf{x}} \\ \bar{\mathbf{u}} \end{bmatrix} = \begin{bmatrix} \mathbf{0} & -\mathbf{M} \\ \mathbf{I} & \mathbf{0} \end{bmatrix} \begin{bmatrix} \bar{\mathbf{z}}_{\mathbf{ref}} \\ \bar{\mathbf{d}} \end{bmatrix}, \quad \Gamma = \begin{bmatrix} \mathbf{A} & \mathbf{B} \\ \mathbf{HC} & \mathbf{0} \end{bmatrix} \in \mathbb{R}^{3N \times 3N} \tag{7}$$

Proposition 1: Given $\bar{\mathbf{z}}_{\mathbf{ref}}$ and $\bar{\mathbf{d}}$, vectors $\bar{\mathbf{x}}$ and $\bar{\mathbf{u}}$ satisfying (7) always exist.

For the proof of this Proposition 1, we defer the reader to [18]. As shown in Figure 2, the dynamics of the integrators

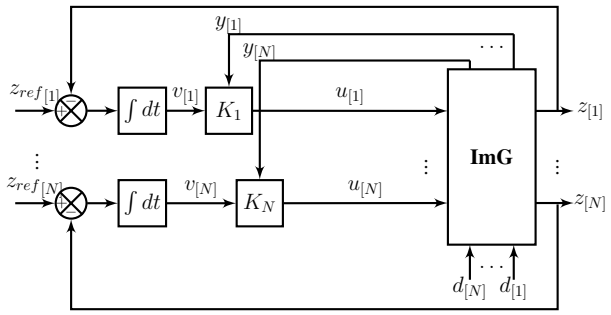

Fig. 2: Control scheme with integrators for the overall augmented microgrid model.

is

$$\dot{v}_{[i]}(t) = e_{[i]}(t) = z_{ref\,[i]}(t) - z_{[i]}(t) = z_{ref\,[i]}(t) - H_i C_i x_{[i]}(t) \tag{8}$$

Therefore, the DGU model augmented with integrators (particularly $\hat{\Sigma}_{[i]}^{DGU}$) can be written as follows

$$\begin{aligned} \dot{\hat{x}}_{[i]}(t) &= \hat{A}_{ii}\hat{x}_{[i]}(t) + \hat{B}_i u_{[i]}(t) + \hat{M}_i \hat{d}_{[i]}(t) + \hat{\xi}_{[i]}(t) \\ \hat{y}_{[i]}(t) &= \hat{C}_i \hat{x}_{[i]}(t) \\ z_{[i]}(t) &= \hat{H}_i \hat{y}_{[i]}(t) \end{aligned} \tag{9}$$

where $\hat{x}_{[i]} = [x^T{}_{[i]}, v_{i,}]^T \in \mathbb{R}^3$ is the state, $\hat{y}_{[i]} = \hat{x}_{[i]} \in \mathbb{R}^3$ is the measurable output, $\hat{d}_{[i]} = [d_{[i]}, z_{ref\,[i]}]^T \in \mathbb{R}^2$ collects the exogenous signals (both current of the load and reference signals) and $\hat{\xi}_{[i]}(t) = \sum_{j \in \mathcal{N}_i} \hat{A}_{ij}\hat{x}_{[j]}(t)$. Combining model $\Sigma_{[i]}^{DGU}$ and (8), one obtains matrices in (9).

By virtue of the next proposition, we make sure that the pair $(\hat{A}_{ii}, \hat{B}_i)$ is controllable, thus system (9) can be stabilized.

Proposition 2: The pair $(\hat{A}_{ii}, \hat{B}_i)$ is controllable.

The proof of Proposition 2 is given in [18].

Recalling (9), we get the overall augmented system as

$$\begin{cases} \dot{\hat{\mathbf{x}}}(t) = \hat{\mathbf{A}}\hat{\mathbf{x}}(t) + \hat{\mathbf{B}}\mathbf{u}(t) + \hat{\mathbf{M}}\hat{\mathbf{d}}(t) \\ \hat{\mathbf{y}}(t) = \hat{\mathbf{C}}\hat{\mathbf{x}}(t) \\ \mathbf{z}(t) = \hat{\mathbf{H}}\hat{\mathbf{y}}(t) \end{cases} \tag{10}$$

where $\hat{\mathbf{x}}$ is the vector of variables $\hat{x}_{[i]}$, $\hat{\mathbf{y}}$ collects variables $\hat{y}_{[i]}$ while $\hat{\mathbf{d}}$ contains variables $\hat{d}_{[i]}$. Matrices $\hat{\mathbf{A}}, \hat{\mathbf{B}}, \hat{\mathbf{C}}, \hat{\mathbf{M}}$ and $\hat{\mathbf{H}}$ are obtained from systems (9).

B. Decentralized PnP control

This section presents the adopted control approach that allows us to design local controlles while guaranteeing asymptotic stability for the augmented system (10). Local controllers are synthesized in a decentralized fashion permitting PnP operations.

We equip each DGU $\hat{\Sigma}_{[i]}^{DGU}$ with the following state-feedback controller

$$\mathcal{C}_{[i]}: \qquad u_{[i]}(t) = K_i \hat{y}_{[i]}(t) = K_i \hat{x}_{[i]}(t) \tag{11}$$

where $K_i \in \mathbb{R}^{1\times 3}$ and controllers $\mathcal{C}_{[i]}$, $i \in \mathcal{D}$ are decentralized since $u_{[i]}(t)$ depends on the state of $\hat{\Sigma}_{[i]}^{DGU}$ only. Moreover, we assume that nominal subsystems are given by $\hat{\Sigma}_{[i]}^{DGU}$ without coupling terms $\hat{\xi}_{[i]}(t)$. From Lyapunov theory, we know that if there exists a symmetric matrix $P_i \in \mathbb{R}^{3\times 3}, P_i > 0$ such that

$$(\hat{A}_{ii} + \hat{B}_i K_i)^T P_i + P_i(\hat{A}_{ii} + \hat{B}_i K_i) < 0, \tag{12}$$

then the nominal closed-loop subsystem equipped with controller $\mathcal{C}_{[i]}$ is asymptotically stable. Similarly, the closed-loop QSL-ImG given by (9) and (11) is asymptotically stable if matrix $\mathbf{P} = \text{diag}(P_1, \ldots, P_N)$ satisfies

$$(\hat{\mathbf{A}} + \hat{\mathbf{B}}\mathbf{K})^T \mathbf{P} + \mathbf{P}(\hat{\mathbf{A}} + \hat{\mathbf{B}}\mathbf{K}) < 0 \tag{13}$$

where $\hat{\mathbf{A}}$, $\hat{\mathbf{B}}$ and $\mathbf{K}$ collect matrices $\hat{A}_{ij}$, $\hat{B}_i$ and K_i, for all $i,\ j \in \mathcal{D}$. We want to emphasize that, in general, (12) does not imply (13), since one can show that decentralized design of local controllers is not sufficient to guarantee voltage stability of the whole ImG, if coupling among DGUs is neglected (see Appendix B in [4] for an example in the case of AC ImGs). In order to derive conditions such that (12) ensures (13), we first define $\hat{\mathbf{A}}_{\mathbf{D}} = \text{diag}(\hat{A}_{ii}, \ldots, \hat{A}_{NN})$ and $\hat{\mathbf{A}}_{\mathbf{C}} = \hat{\mathbf{A}} - \hat{\mathbf{A}}_{\mathbf{D}}$. Then, we exploit the following assumptions to obtain asymptotic stability of the closed-loop QSL-ImG.

Assumption 2: (i) Decentralized controllers $\mathcal{C}_{[i]}$, $i \in \mathcal{D}$ are designed such that (12) holds with

$$P_i = \left(\begin{array}{c|cc} \eta_i & 0 & 0 \\ \hline 0 & \bullet & \bullet \\ 0 & \bullet & \bullet \end{array}\right) \tag{14}$$

where $\bullet$ denotes an arbitrary entry and $\eta_i > 0$ is a local parameter.

(ii) It holds $\frac{\eta_i}{R_{ij}C_{ti}} \approx 0$, $\forall i \in \mathcal{D}$, $\forall j \in \mathcal{N}_i$.

As regards Assumption 2-(i), we will show later that checking the existence of P_i as in (14) and K_i fulfilling (12) leads to solving a convex optimization problem. On the other hand, to fulfill Assumption 2-(ii), when an upper bound to all ratios $\frac{1}{R_{ij}C_{ti}}$ (which depend upon line parameters only) is known, one can simply set the control design parameter η_i sufficiently small.

Proposition 3: Let Assumption 2 holds. Then, the overall closed-loop QSL-ImG is asymptotically stable.

The proof of Proposition 3 is presented in [18].

At this point, in order to complete the design of the local controller $\mathcal{C}_{[i]}$, we have to solve the following problem.

Problem 1: Compute a matrix K_i such that the nominal closed-loop subsystem is asymptotically stable and Assumption 2-(i) is verified, i.e. (12) holds for a matrix P_i structured as in (14).

Consider the following optimization problem

$$\mathcal{O}_i : \min_{Y_i, G_i, \gamma_i, \beta_i, \delta_i} \quad \alpha_{i1}\gamma_i + \alpha_{i2}\beta_i + \alpha_{i3}\delta_i$$

$$Y_i = \begin{bmatrix} \eta_i^{-1} & 0 & 0 \\ 0 & \bullet & \bullet \\ 0 & \bullet & \bullet \end{bmatrix} > 0 \tag{15a}$$

$$\begin{bmatrix} Y_i \hat{A}_{ii}^T + G_i^T \hat{B}_i^T + \hat{A}_{ii} Y_i + \hat{B}_i G_i & Y_i \\ Y_i & -\gamma_i I \end{bmatrix} \leq 0 \tag{15b}$$

$$\begin{bmatrix} -\beta_i I & G_i^T \\ G_i & -I \end{bmatrix} < 0 \tag{15c}$$

$$\begin{bmatrix} Y_i & I \\ I & \delta_i I \end{bmatrix} > 0 \tag{15d}$$

$$\gamma_i > 0, \quad \beta_i > 0, \quad \delta_i > 0 \tag{15e}$$

where α_{i1}, α_{i2} and α_{i3} represent positive weights and $\bullet$ are arbitrary entries. Problem (15) is an LMI problem, i.e. an optimization problem for which polynomial-time solvers exist [19].

Lemma 1: Problem $\mathcal{O}_i$ is feasible if and only if Problem 1 has a solution. Moreover, K_i and P_i in (12) are given by $K_i = G_i Y_i^{-1}$, $P_i = Y_i^{-1}$ and $||K_i||_2 < \sqrt{\beta_i}\delta_i$.
The proof of Lemma 1 is given in [18].

Next, we discuss the key feature of the proposed decentralized control approach. We first notice that constraints in (15) depend upon local fixed matrices ($\hat{A}_{ii}$, $\hat{B}_i$) and local design parameters (α_{i1}, α_{i2}, α_{i3}). It follows that the computation of controller $\mathcal{C}_{[i]}$ is independent from the computation of controllers $\mathcal{C}_{[j]}$ when $j \neq i$. In addition, constraints (15c) and (15d) affect only the magnitude of control variables (see the proof of Lemma 1 in [18]).

In order to improve transient performances of controllers $\mathcal{C}_{[i]}$, pre-filters of reference signals ($\tilde{C}_{[i]}$) and local compensator of measurable disturbances ($N_{[i]}$) can be incorporated to each subsystem. These customary steps in control design are detailed in Section 3.3 of [18].

Algorithm 1 summarizes the whole design procedure.

Algorithm 1 Design of controller $\mathcal{C}_{[i]}$ and compensators $\tilde{C}_{[i]}$ and $N_{[i]}$ for subsystem $\hat{\Sigma}_{[i]}^{DGU}$

Input: DGU $\hat{\Sigma}_{[i]}^{DGU}$ as in (9)

Output: Controller $\mathcal{C}_{[i]}$ and, optionally, pre-filter $\tilde{C}_{[i]}$ and compensator $N_{[i]}$

(A) Find K_i solving the LMI problem (15). If it is not feasible **stop** (the controller $\mathcal{C}_{[i]}$ cannot be designed).
Optional steps
(B) Design the asymptotically stable local pre-filter $\tilde{C}_{[i]}$ and compensator $N_{[i]}$ (see Section 3.3 of [18]).

C. PnP operations

In the following section, the operations for updating the controllers when DGUs are added to or removed from an ImG are presented. We remind that all these operations must be performed while preserving stability of the new closed-loop system. Consider, as a starting point, an ImG composed of subsystems $\hat{\Sigma}_{[i]}^{DGU}, i \in \mathcal{D}$ equipped with local controllers $\mathcal{C}_{[i]}$ and compensators $\tilde{C}_{[i]}$ and $N_{[i]}$, $i \in \mathcal{D}$ produced by Algorithm 1.

Remark 1: In order to avoid jumps in the control variable when local regulator are switched, we embedded each local regulator into a bumpless control scheme [20] described in Appendix B of [18].

Plugging-in operation Assume that the plug-in of a new DGU $\hat{\Sigma}_{[N+1]}^{DGU}$ described by matrices, $\hat{A}_{N+1\,N+1}$, $\hat{B}_{N+1}$, $\hat{C}_{N+1}$, $\hat{M}_{N+1}$, $\hat{H}_{N+1}$ and $\{\hat{A}_{N+1\,j}\}_{j\in\mathcal{N}_{N+1}}$ needs to be performed. Let $\mathcal{N}_{N+1}$ be the set of DGUs that are directly coupled to $\hat{\Sigma}_{[N+1]}^{DGU}$ through transmission lines and let $\{\hat{A}_{N+1\,j}\}_{j\in\mathcal{N}_{N+1}}$ be the matrices containing the corresponding coupling terms. According to our method, the design of controller $\mathcal{C}_{[N+1]}$ and compensators $\tilde{C}_{[N+1]}$ and $N_{[N+i]}$ requires Algorithm 1 to be executed. Since DGUs $\hat{\Sigma}_{[j]}^{DGU}$, $j \in \mathcal{N}_{N+1}$, have the new neighbour $\hat{\Sigma}_{[N+1]}^{DGU}$, we need to redesign controllers $\mathcal{C}_{[j]}$ and compensators $\tilde{C}_{[j]}$ and $N_{[j]}$, $\forall j \in \mathcal{N}_{N+1}$ because matrices $\hat{A}_{jj}$, $j \in \mathcal{N}_{N+1}$ change.

Only if Algorithm 1 does not stop in Step A when computing controllers $\mathcal{C}_{[k]}$ for all $k \in \mathcal{N}_{N+1} \cup \{N+1\}$, we have that the plug-in of $\hat{\Sigma}_{[N+1]}^{DGU}$ is allowed. Moreover, we stress that the redesign is not propagated further in the network and therefore the asymptotic stability of the new overall closed-loop QSL-ImG model is preserved even without changing controllers $\mathcal{C}_{[i]}$, $\tilde{C}_{[i]}$ and $N_{[i]}$, $i \notin \{N+1\} \cup \mathcal{N}_{N+1}$.

Prior to real-time plugging-in operation (*hot plugging-in*), it is recommended to keep set points constant for a sufficient amount of time so as to guarantee control variable in the bumpless control scheme (see Remark 1) is in steady state. This ensures smooth behaviours of the electrical variables.

Unplugging operation Let us now examine the unplugging of DGU $\hat{\Sigma}_{[k]}^{DGU}$, $k \in \mathcal{D}$. The disconnection of $\hat{\Sigma}_{[k]}^{DGU}$ from the network leads to a change in matrix $\hat{A}_{jj}$ of each $\hat{\Sigma}_{[j]}^{DGU}$, $j \in \mathcal{N}_k$. Consequently, for each $j \in \mathcal{N}_k$, we have to redesign controllers $\mathcal{C}_{[j]}$ and compensators $\tilde{C}_{[j]}$ and $N_{[j]}$. As for the plug-in operation, we run Algorithm 1. If all operations can be successfully terminated, then the unplugging of $\hat{\Sigma}_{[k]}^{DGU}$ is allowed and stability is preserved without redesigning the local controllers $\mathcal{C}_{[j]}$, $j \notin \mathcal{N}_k$.

When an unplugging operation is scheduled in advance, it is advisable to follow an *hot unplugging* protocol similar to the one introduced for the plugging-in operation.

IV. Simulation results

In this section, we study performance brought about by PnP controllers described in Section III by using the ImG in Figure 1 with two DGUs (Scenario 1) and an ImG with 6 DGUs (Scenario 2). Simulations have been performed in PSCAD, a simulation environment for electric systems which allows to implement the microgrid model with realistic electric components. For both scenarios, we run a simulation from time 0 s up to time 10 s. Each simulation has been split into subparts that are discussed next.

A. Scenario 1

In this Scenario, we consider the ImG shown in Figure 1 composed of two DGUs connected through high resistive-inductive lines supporting 10 Ω and 6 Ω loads, respectively. For the sake of simplicity, we set $i = 1$ and $j = 2$. The output voltage reference $v^{\star}_{MG}$ has been selected at 48 V for both DGUs. Parameters values for all DGUs are given in Table 1 of [18] and they are comparable to those used in [5].

1) Voltage reference tracking at the startup: We assume that at the beginning of the simulation ($t = 0$ s), subsystems $\hat{\Sigma}^{DGU}_{[1]}$ and $\hat{\Sigma}^{DGU}_{[2]}$ are not interconnected. Therefore, stabilizing controllers $\mathcal{C}_i$, $i = 1, 2$ are designed neglecting coupling among DGUs. Moreover, in order to widen the bandwidth of each closed-loop subsystem, we use local pre-filters $\tilde{C}_{[i]}$, $i = 1, 2$ of reference signals (see Figure 5 of [18]). The desired transfer functions $\tilde{F}_i(s)$, $i = 1, 2$ have been chosen as low-pass filters with DC gain equal to 0 dB and bandwidth equal to 100 Hz. Figures 3a and 3b show the voltages at PCC_1 and PCC_2. Note that the controllers ensure an excellent tracking of the reference signals at the startup in a very short time.

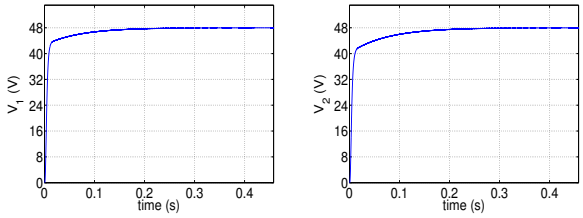

(a) Load voltage at PCC_1. (b) Load voltage at PCC_2.

Fig. 3: Scenario 1 - Voltage reference tracking at the startup.

2) Hot plugging-in of DGUs 1 and 2: At time $t = 2$ s, we connect DGUs 1 and 2 together. This requires real-time switch of the local controllers which translates into two hot plugging-in operations as described in Section III-C. The new decentralized controllers for subsystems $\hat{\Sigma}^{DGU}_{[1]}$ and $\hat{\Sigma}^{DGU}_{[2]}$ are designed running Algorithm 1. Notice that the interconnection of the two subsystems leads to a variation of each DGU dynamics, therefore even compensators $\tilde{C}_{[i]}$ and $N_{[i]}$, $i = 1, 2$ need to be updated. In particular, the new desired closed-loop transfer functions $\tilde{F}_i(s)$, $i = 1, 2$ have been chosen as low-pass filters with DC gain equal to 0 dB and bandwidth equal to 100 Hz.

Since Algorithm 1 never stops in Step A, the hot plug-in of the DGUs is allowed and local controllers get replaced by the new ones at $t = 2$ s. Bode plots of the compensators and the closed-loop system are given in Figure 7 of [18].

Figure 4 shows the dynamic responses of the voltages at PCC_1 and PCC_2 when the subsystems are connected together. We highlight that the bumpless control transfer schemes ensure no significant deviations in the output signals when the controller switch is performed. Moreover, through the proposed decentralized control strategy, voltage regulation is excellent.

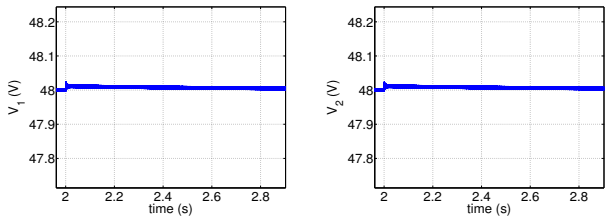

(a) Load voltage at PCC_1. (b) Load voltage at PCC_2.

Fig. 4: Scenario 1 - Impact of bumpless control transfer on the hot plug-in at time $t = 2$ s.

B. Scenario 2

In this second scenario, we consider the meshed ImG depicted in black in Figure 5. However, differently from Scenario 1, some DGUs have more than one neighbour and hence the disturbances that will influence their dynamics will be greater. It is also present a loop that further complicates voltage regulation. To our knowledge, control of loop-interconnected DGUs has never been investigated for DC microgrids. We consider DGUs with non-identical electrical parameters (given in Tables 2, 3 and 4 of [18]). We also assume that DGUs 1-5 supply 10 Ω, 6 Ω, 20 Ω, 2 Ω and 4 Ω loads, respectively. Moreover, for this Scenario, no compensators $\tilde{C}_i$ and N_i have been used. At the beginning of the simulation, all the DGUs are assumed to be isolated and not connected to each other. However, we choose to equip each subsystem $\hat{\Sigma}^{DGU}_{[i]}$, $i \in \mathcal{D} = \{1, \ldots, 5\}$, with controllers $\mathcal{C}_{[i]}$ designed by running Algorithm 1 and taking into account couplings among DGUs. This is possible because, as shown in Section III-B, local controllers stabilize the ImG also in absence of couplings. Because of this choice of local controllers in the startup phase, when the five subsystems are connected together at time $t = 1.5$ s, no bumpless control scheme is required since no real-time switch of controllers is performed.

For evaluating the PnP capabilities of our control approach, we simulate the connection of DGU $\hat{\Sigma}^{DGU}_{[6]}$ with $\hat{\Sigma}^{DGU}_{[1]}$ and $\hat{\Sigma}^{DGU}_{[5]}$, as shown in Figure 5. Therefore, we have $\mathcal{N}_6 = \{1, 5\}$. In principle, subsystems $\hat{\Sigma}^{DGU}_{[j]}$, $j \in \mathcal{N}_6$ must update their controllers $\mathcal{C}_{[j]}$ (see Section III-C). However, we highlight that previous controllers for DGUs $\hat{\Sigma}^{DGU}_{[1]}$ and $\hat{\Sigma}^{DGU}_{[5]}$ can be also maintained, provided that the already computed matrices K_j, $j \in \mathcal{N}_6$ still fulfill all constraints in (15) for the new ImG topology. Since this test succeeds, we proceed by executing Algorithm 1 for synthesizing $\mathcal{C}_{[6]}$ for the new DGU only. Algorithm 1 never stops in Step A and therefore the addition of $\hat{\Sigma}^{DGU}_{[6]}$ is allowed.

The real-time plugging-in of $\hat{\Sigma}^{DGU}_{[6]}$ is executed at time $t = 2$ s. Until the plug-in of $\hat{\Sigma}^{DGU}_{[6]}$, common reference $v^{\star}_{MG}$ for DGUs 1-5 is the same as for DGUs 1-2 in Scenario 1 and the subsystem $\hat{\Sigma}^{DGU}_{[6]}$ is assumed to work isolated, tracking the reference voltage $v^{\star}_{MG}$. We note that right after the hot plug-in of $\hat{\Sigma}^{DGU}_{[6]}$ at $t = 2$ s, load voltages of $\hat{\Sigma}^{DGU}_{[1]}$ and

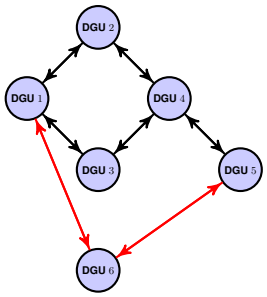

Fig. 5: Scenario 2 - Scheme of the ImG composed of 6 DGUs (in black) and plugging-in of $\hat{\Sigma}_{[6]}^{DGU}$ (in red).

$\hat{\Sigma}_{[5]}^{DGU}$ do not deviate from the respective reference signals (see Figure 15 in [18]). In order to test the robustness of the overall ImG to unknown load dynamics, at $t = 3$ s we halve the load of DGU 6, which was equal to 8 Ω for $t < 3$ s. Figures 6a and 6b show that, when the load change of $\hat{\Sigma}_{[6]}^{DGU}$ occurs, the voltages at PCC_1 and PCC_5 exhibit very small variations which last for a short time. Then, load voltages of $\hat{\Sigma}_{[1]}^{DGU}$ and $\hat{\Sigma}_{[5]}^{DGU}$ converge to their reference values. Similar remarks can be done for the new DGU $\hat{\Sigma}_{[6]}^{DGU}$: as shown in Figure 6c, there is a short transient at the time of the load change, that is effectively compensated by the control action. These experiments highlight that controllers $\mathcal{C}_{[i]}$, $i = 1, \ldots, 6$ may ensure very good tracking of the reference signal and robustness to unknown load dynamics even without using compensators $\tilde{C}_{[6]}$ and $N_{[6]}$.

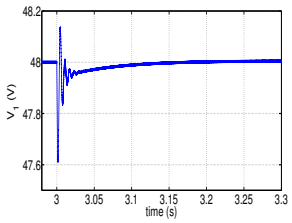

(a) Voltage at PCC_1.

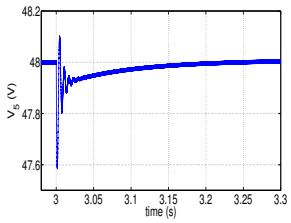

(b) Voltage at PCC_5.

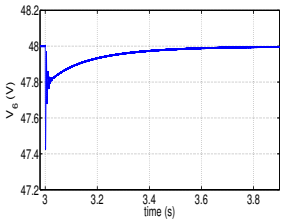

(c) Voltage at PCC_6.

Fig. 6: Scenario 2 - Performance of PnP decentralized voltage controllers in terms of robustness to an abrupt change of load resistances at time $t = 3$ s.

Moreover, in Section 4.2.3 of [18], we demonstrate good performance of PnP controllers when a DGU is disconnected at a certain time.

V. Conclusions

This paper presented a decentralized control scheme for guaranteeing voltage stability in DC ImGs when DGUs are plugged in or out. Future research will consider extensions to general interconnections of DGUs and loads as well as coupling of PnP controllers with a secondary control layer devoted to current sharing.

References

[1] R. Lasseter, A. Akhil, C. Marnay, J. Stephens, J. Dagle, R. Guttromson, A. Meliopoulous, R. Yinger, and J. Eto, "The certs microgrid concept," *White paper for Transmission Reliability Program, Office of Power Technologies, US Department of Energy*, 2002.

[2] J. M. Guerrero, M. Chandorkar, T.-L. Lee, and P. C. Loh, "Advanced control architectures for intelligent microgrids - part I: decentralized and hierarchical control," *IEEE Transactions on Industrial Electronics*, vol. 60, no. 4, pp. 1254–1262, 2013.

[3] S. Riverso, F. Sarzo, and G. Ferrari-Trecate, "Plug-and-play voltage and frequency control of islanded microgrids with meshed topology," *IEEE Transactions on Smart Grid*, vol. 6, no. 3, pp. 1176–1184, 2015.

[4] ——, "Plug-and-play voltage and frequency control of islanded microgrids with meshed topology," Tech. Rep., 2014. [Online]. Available: arXiv:1405.2421

[5] Q. Shafiee, T. Dragičević, J. C. Vasquez, and J. M. Guerrero, "Modeling, Stability Analysis and Active Stabilization of Multiple DC-Microgrid Clusters," in *Proceedings of the IEEE ENERGYCON*, 2014, pp. 1284–1290.

[6] A. T. Elsayed, A. A. Mohamed, and O. A. Mohammed, "Dc microgrids and distribution systems: An overview," *Electric Power Systems Research*, vol. 119, pp. 407–417, 2015.

[7] J. W. Simpson-Porco, F. Dörfler, and F. Bullo, "Synchronization and power sharing for droop-controlled inverters in islanded microgrids," *Automatica*, vol. 49, no. 9, pp. 2603–2611, 2013.

[8] A. H. Etemadi, E. J. Davison, and R. Iravani, "A decentralized robust control strategy for multi-der microgrids part I: Fundamental concepts," *IEEE Transactions on Power Delivery*, vol. 27, no. 4, pp. 1843–1853, 2012.

[9] S. Riverso, M. Farina, and G. Ferrari-Trecate, "Plug-and-Play Decentralized Model Predictive Control for Linear Systems," *IEEE Transactions on Automatic Control*, vol. 58, no. 10, pp. 2608–2614, 2013.

[10] ——, "Plug-and-Play Model Predictive Control based on robust control invariant sets," *Automatica*, vol. 50, no. 8, pp. 2179–2186, 2014.

[11] S. Riverso, "Distributed and plug-and-play control for constrained systems," Ph.D. dissertation, 2014. [Online]. Available: http://sisdin.unipv.it/pnpmpc/phpinclude/papers/phd_thesis_riverso.pdf

[12] J. Stoustrup, "Plug & play control: Control technology towards new challenges," *European Journal of Control*, vol. 15, no. 3, pp. 311–330, 2009.

[13] X. Lu, J. M. Guerrero, K. Sun, and J. C. Vasquez, "An improved droop control method for dc microgrids based on low bandwidth communication with dc bus voltage restoration and enhanced current sharing accuracy," *IEEE Transactions on Power Electronics*, vol. 29, no. 4, pp. 1800–1812, 2014.

[14] J. Zhao and F. Drfler, "Distributed control, load sharing, and dispatch in dc microgrids," in *American Control Conference*, 2015.

[15] M. Andreasson, D. V. Dimarogonas, H. Sandberg, and K. H. Johansson, "Distributed controllers for multi-terminal hvdc transmission systems," *arXiv preprint arXiv:1411.1864*, 2014.

[16] V. Venkatasubramanian, H. Schattler, and J. Zaborszky, "Fast Time-Varying Phasor Analysis in the Balanced Three-Phase Large Electric Power System," *IEEE Transactions on Automatic Control*, vol. 40, no. 11, pp. 1975–1982, 1995.

[17] M. Babazadeh and H. Karimi, "A Robust Two-Degree-of-Freedom Control Strategy for an Islanded Microgrid," *IEEE Transactions on Power Delivery*, vol. 28, no. 3, pp. 1339–1347, 2013.

[18] M. Tucci, S. Riverso, J. C. Vasquez, J. M. Guerrero, and G. Ferrari-Trecate, "A decentralized scalable approach to voltage control of DC islanded microgrids," Tech. Rep., 2015. [Online]. Available: arXiv:1503.06292

[19] S. Boyd, L. El Ghaoui, E. Feron, and V. Balakrishnan, *Linear matrix inequalities in system and control theory*. Philadelphia, Pennsylvania, USA: SIAM Studies in Applied Mathematics, vol. 15, 1994.

[20] K. J. Åström and T. Hägglund, *Advanced PID control*. ISA-The Instrumentation, Systems, and Automation Society; Research Triangle Park, NC 27709, 2006.